2416 *Inorg. Chem.* **2010**, *49*, 2416–2426
DOI: 10.1021/ic902311g

Inorganic Chemistry
Article

Synthesis and Characterization of New Coordination Polymers with Tunable Luminescent Properties Generated from Bent 1,2,4-Triazole-Bridged *N,N′*-Dioxides and Ln(III) Salts

Hai-Ying Wang, Jun-Yan Cheng, Jian-Ping Ma, Yu-Bin Dong,* and Ru-Qi Huang

College of Chemistry, Chemical Engineering and Materials Science, Key Lab of Molecular and Nano Probe, Engineering Research Center of Pesticide and Medicine Intermediate Clean Production, Ministry of Education, Shandong Normal University, Jinan, 250014, P. R. China

Received November 23, 2009

A new bent 1,2,4-triazole-bridged *N,N′*-dioxide ligand, namely, 3,5-bis(3-pyridyl-*N*-oxide)-4-amino-1,2,4-triazole (**L2**), was designed and synthesized by the oxidation of 3,5-bis(3-pyridyl)-4-amino-1,2,4-triazole with H_2O_2 in the presence of HOAc at ambient temperatures. Eleven Ln(III)-based coordination polymers have been successfully prepared by the solution reactions of **L2** with various Ln(III)−perchlorates. The structures of these new Ln(III) polymers clearly reflect the effect of the lanthanide contraction. Compounds **1**−**6** feature a two-dimensional net, in which the Ln(III) atoms adopt a nine-coordinate $\{LnO_9\}$ sphere due to their larger ionic radii, whereas the Ln(III) centers in the one-dimensional double-stranded chains of **7**−**11** with smaller ionic radii lie in a $\{LnO_8\}$ coordination environment. In addition, the tunable emission intensity was realized on **7** by controlling the type of the involved counterion on the basis of a reversible solid-state anion exchange. Such reversible solid-state anion exchange might provide an alternative approach to tuning the luminescence.

Introduction

Due to their interesting luminescent and magnetic properties, the lanthanide-series-based coordination polymers are likely to provide new materials that possess specific properties and desired features.[1] As we know, self-assembly of organic ligands and lanthanide cations is currently the most efficient and widely utilized approach for the construction of discrete and polymeric lanthanide-based coordination complexes.[2] Compared to the N-donor ligands, organic molecules possessing oxygen donors such as −COOH, >C═O, −OH, and −CONH groups are the generally preferred choice to link lanthanide cations into coordination compounds because of the complementarity of the hard metal cationic acid and hard donor base. Over the past decades, numerous elaborate lanthanide-based coordination polymers based on such organic spacers have been successfully synthesized; the lanthanide coordination polymers generated from the *N,N′*-dioxides, however, have attracted much less attention,[3] probably due to the inherent difficulty in the synthesis of *N*-oxide organic ligands which is usually required in a strong oxidation process.

Recently, our research group has provided a series of bent symmetric and unsymmetric rigid and flexible organic pyridine, benzonitrile, phenylamine, Schiff-base, and carboxylate ligands bridged by the five-membered heterocyclic rings for assembly of discrete and polymeric metal-organic frameworks.[4] Our systemic study demonstrates that the bent geometries of these ligands are capable of generating metal-organic coordination patterns not easily achievable by linear ligands. This alternative ligand-directed approach did result in some novel coordination metal-organic frameworks, especially the molecular containers with a well-isolated cavity. Moreover, heteroatoms such as N and O with free electron

*To whom correspondence should be addressed. E-mail: yubindong@sdnu.edu.cn.

(1) (a) Aspinall, H. C. *Chem. Rev.* **2002**, *102*, 1807. (b) Shibasaki, M.; Yoshikawa, N. *Chem. Rev.* **2002**, *102*, 2187. (c) Bünzli, J.-C. G.; Piguet, C. *Chem. Rev.* **2002**, *102*, 1897. Kido, J.; Okamoto, Y. *Chem. Rev.* **2002**, *102*, 2357. (d) Inanga, J.; Furuno, H.; Hayano, T. *Chem. Rev.* **2002**, *102*, 2211. (e) Tsukube, H.; Shinoda, S. *Chem. Rev.* **2002**, *102*, 2389.

(2) (a) Bretonnière, Y.; Mazzanti, M.; Pécaut, J.; Olmstead, M. M. *J. Am. Chem. Soc.* **2002**, *124*, 9012. (b) Hamacek, J.; Blanc, S.; Elhabiri, M.; Leize, E.; Dorsselaer, A. V.; Piguet, C.; Albrecht-Gary, A.-M. *J. Am. Chem. Soc.* **2003**, *125*, 1514. (c) Cheng, J.-W.; Zhang, J.; Zheng, S.-T.; Zhang, M.-B.; Yang, G.-Y. *Angew. Chem., Int. Ed.* **2006**, *45*, 73. (d) Gándara, F.; Perles, J.; Snejko, N.; Lglesias, M.; Gómez-Lor, B.; Gutiérrez-Puebla, E.; Monge, M. Á. *Angew. Chem., Int. Ed.* **2006**, *45*, 7998. (e) Devic, T.; David, O.; Valls, M.; Marrot, J.; Couty, F.; Férey, G. *J. Am. Chem. Soc.* **2007**, *129*, 12614. (f) Li, X.; Liu, W.; Guo, Z.; Tan, M. *Inorg. Chem.* **2003**, *42*, 8735. (g) Ma, L.; Evans, O.; Foxman, B. M.; Lin, W. *Inorg. Chem.* **1999**, *38*, 5837. (h) Black, C. A.; Costa, J. S.; Fu, W. T.; Massera, C.; Roubeau, O.; Teat, S. J.; Aromí, G.; Gamez, P.; Reedijk, J. *Inorg. Chem.* **2009**, *48*, 1062.

(3) (a) Hill, R. J.; Long, D.-L.; Champness, N. R.; Hubberstey, P.; Schröder, M. *Acc. Chem. Res.* **2005**, *38*, 337. (b) Loeb, S. J. *Chem. Commun.* **2005**, 1511. (c) Hiffart, D. J.; Loeb, S. J. *Angew. Chem., Int. Ed.* **2005**, *44*, 901. (d) Zhang, L.-P.; Lu, W.-J.; Mak, T. C. W. *Chem. Commun.* **2003**, 2830.

 Published on Web 01/26/2010

pairs on the central heterocyclic bridges can be considered as potential active coordination sites and/or hydrogen bond acceptors to bind guest species through these weak interactions, sometimes in a reversible manner. Motivated by this, we have initiated a synthetic program for the preparation of supramolecular assembly, in which the symmetric and asymmetric bent *N*,*N*′-dioxide spacers linked by five-membered heteroatom rings are chosen as the building blocks. In this contribution, we report a new bent *N*,*N*′-dioxide-type ligand, namely, 3,5-bis(3-pyridyl-*N*-oxide)-4-amino-1,2,4-triazole, and a series of lanthanide coordination polymers based on it. Additionally, we found that the luminescent intensities of the lanthanide coordination polymers can be tuned by controlling the involved counterions.

Experimental Section

Materials and Methods. Lanthanide salts (Acros) were used as obtained without further purification. Infrared (IR) samples were prepared as KBr pellets, and spectra were obtained in the 400−4000 cm^{-1} range using a Perkin-Elmer 1600 FTIR spectrometer. Elemental analyses were performed on a Perkin-Elmer model 2400 analyzer. ^{1}H NMR data were collected using an AM-300 spectrometer. Chemical shifts are reported in δ relative to TMS. All fluorescence measurements were carried out on a Cary Eclipse Spectrofluorimeter (Varian, Australia) equipped with a xenon lamp and quartz carrier at room temperature. XRD patterns were obtained on a D8 ADVANCE X-ray powder diffraction (XRD) apparatus with Cu Kα radiation (λ = 1.5405 and A ring).

Caution! *The crystallization procedures involve lanthanide perchlorate, which is a strong oxidizer.*

Preparation of L2. A mixture of L1[5] (3.17 g, 13 mmol), a 30% hydrogen peroxide solution (1.8 mL), and acetic acid (9.4 mL) was refluxed at 70−80 °C for 36 h. After removal of the solvent under a vacuum, the residue was purified on a silica gel column using CH_2Cl_2/CH_3OH (4:1, v/v) as the eluent to afford **L2** as a light pink crystalline solid (1.46 g, yield: 38%). Mp = 320−323 °C. IR (KBr pellet cm^{-1}): 3328(ms), 3080(ms), 1603(ms), 1567(ms), 1472(s), 1438(ms), 1312(ms), 1285(ms), 1245(ms), 1220(s), 1141(ms), 1099(w), 1015(s), 938(w), 893(s), 808(ms), 717(w), 672(w), 629(w), 552(ms), 501(ms), 438(ms), 419(w). ^{1}H NMR (300 MHz, DMSO, 25 °C, TMS, ppm): 8.88 (s, 2H, C_5H_4N), 8.38 (d, 2H, C_5H_4N), 7.93 (d, 2H, C_5H_4N), 7.61 (t, 3H, C_5H_4N), 6.52 (s, 2H, NH_2). Elem anal. (%) calcd for $C_{12}H_{10}N_6O_2$: C 53.33, H 3.70, N 31.11. Found: C 53.29, H 3.51, N 30.84. The asymmetric oxidation product **L3** was collected as a light pink crystalline solid in 12% yield (0.37 g). Mp = 305−307 °C. IR (KBr pellet cm^{-1}): 3325(m), 3194(w), 3060(m), 1603(m), 1576(m), 1480(m), 1459(s), 1404(w), 1357(w), 1336(w), 1309(w), 1281(w), 1204(vs), 1198(w), 1180(w), 1155(m), 1099(w), 1011(m), 980(m), 936(m), 895(s), 807(m),716(m), 681(m), 631(w), 553(w), 511(m), 481(w), 422(w). ^{1}H NMR (300 MHz, DMSO, 25 °C, TMS, ppm): 9.15 (s, 1H, C_5H_4N), 8.88 (s, 1H, C_5H_4N), 8.71 (d, 1H, C_5H_4N), 8.35 (m, 2H, C_5H_4N), 7.93 (d, 1H, C_5H_4N), 8.35 (t, 2H, C_5H_4N), 6.46 (s, 2H, NH_2). Elem anal. (%) calcd for $C_{12}H_{10}N_6O$: C 56.69, H 3.96, N 33.05. Found: C 56.35, H 3.77, N 32.93.

Preparation of 1. A THF solution (2 mL) of **L2** (13 mg, 0.048 mmol) was gently added to an aqueous solution (2 mL) of $La(ClO_4)_3\cdot 6H_2O$. Upon slow evaporation, colorless block-like crystals (27 mg) were obtained. Yield, 53% (based on **L2**). IR (KBr pellet, cm^{-1}): 3422(vs), 1625(s), 1476(s), 1436(s), 1310(m), 1291(m), 1253(s), 1089(vs), 985(w), 943(s), 912(m), 803(m), 722(m), 665(m), 625(s), 570(m), 482(w). Elem anal. (%) calcd for $C_{24}H_{30}Cl_3N_{12}O_{21}La$: C 26.99, H 2.83, N 15.74. Found: C 26.81, H 2.85, N 15.62.

Preparation of 2. A THF solution (2 mL) of **L2** (26 mg, 0.096 mmol) was gently added to an aqueous solution (2 mL) of $Pr(ClO_4)_3\cdot 6H_2O$ (90 mg). Upon slow evaporation, yellow block-like crystals (46 mg) were obtained. Yield, 45% (based on **L2**). IR (KBr pellet, cm^{-1}): 3368(s), 3106(s), 1624(s), 1518(w), 1476(s), 1436(s), 1353(w), 1310(m), 1292(m), 1251(s), 1089(vs), 985(w), 944(w), 912(s), 803(m), 723(m), 665(m), 622(s), 570(m), 482(w). Elem anal. (%) calcd for $C_{24}H_{30}Cl_3N_{12}O_{21}Pr$: C 26.94, H 2.83, N 15.71. Found: C 26.85, H 2.91, N 15.59.

Preparation of 3. An aqueous solution (5 mL) of **L2** (40 mg, 0.148 mmol) was gently added to an aqueous solution (5 mL) of $Nd(ClO_4)_3\cdot 6H_2O$ (131 mg). Upon slow evaporation, pink block-like crystals (59 mg) were obtained. Yield, 37% (based on **L2**). IR (KBr pellet, cm^{-1}): 3424(vs), 3107(vs), 1624(s), 1477(s), 1436(s), 1310(m), 1292(m), 1251(s), 1088(vs), 911(s), 803(m), 722(m), 665(m), 623(s), 569(m), 482(m). Elem anal. (%) calcd for $C_{24}H_{30}Cl_3N_{12}O_{21}Nd$: C 26.86, H 2.82, N 15.66. Found: C 26.93, H 2.91, N 15.59.

Preparation of 4. An aqueous solution (5 mL) of **L2** (13 mg, 0.048 mmol) was gently added to an aqueous solution (5 mL) of $Sm(ClO_4)_3\cdot 6H_2O$ (26 mg). Upon slow evaporation, colorless block-like crystals (26 mg) were obtained. Yield, 51% (based on **L2**). IR (KBr pellet, cm^{-1}): 3369(s), 1624(m), 1476(s), 1437(s), 1311(w), 1292(w), 1239(s), 1089(vs), 944(w), 910(s), 804(m), 723(m), 667(m), 626(s), 569(m), 482(w). Elem anal. (%) calcd for $C_{24}H_{30}Cl_3N_{12}O_{21}Sm$: C 26.71, H 2.80, N 15.57. Found: C 26.68, H 2.77, N 15.63.

Preparation of 5. A THF solution (2 mL) of **L2** (20 mg, 0.074 mmol) was gently added to an aqueous solution (2 mL) of $Eu(ClO_4)_3\cdot 6H_2O$ (85 mg). Upon slow evaporation, colorless block-like crystals (41 mg) were obtained. Yield, 52% (based on **L2**). IR (KBr pellet, cm^{-1}): 3427(vs), 1624(s), 1519(w), 1476(s), 1437(s), 1353(w), 1312(m), 1293(m), 1249(s), 1089(vs), 945(w), 909(s), 803(m), 723(m), 666(m), 622(s), 568(m), 482(w). Elem anal. (%) calcd for $C_{24}H_{30}C_{13}N_{12}O_{21}Eu$: C 26.67, H 2.80, N 15.55. Found: C 26.76, H 2.93, N 15.49.

Preparation of 6. A THF solution (2 mL) of **L2** (20 mg, 0.074 mmol) was gently added to an aqueous solution (2 mL) of $Gd(ClO_4)_3\cdot 6H_2O$ (77 mg). Upon slow evaporation, yellow block-like crystals (41 mg) were obtained. Yield, 46% (based on **L2**). IR (KBr pellet, cm^{-1}): 3425(vs), 1624(s), 1520(w), 1476(s), 1438(s), 1353(w), 1312(m), 1293(m), 1249(s), 1089(vs), 945(w), 910(s), 804(s), 723(s), 666(s), 622(s), 567(s), 482(m). Elem anal. (%) calcd for $C_{24}H_{30}C_{13}N_{12}O_{21}Gd$: C 26.54, H 2.78, N 15.47. Found: C 26.44, H 2.83, N 15.37.

Preparation of 7. An aqueous solution (5 mL) of **L2** (20 mg, 0.074 mmol) was gently added to an aqueous solution (5 mL) of $Tb(ClO_4)_3\cdot 6H_2O$ (80 mg). Upon slow evaporation, colorless block-like crystals (30 mg) were obtained. Yield, 38% (based on **L2**). IR (KBr pellet, cm^{-1}): 3383(vs), 2023(w), 1651(s), 1523(w), 1490(m), 14706(s), 1413(w), 1362(w), 1296(m), 1238(s), 1215(s),

(4) Some of our research papers on bent five-membered heterocycle bridging ligands: (a) Dong, Y.-B.; Ma, J.-P.; Smith, M. D.; Huang, R.-Q.; Tang, B.; Chen, D.; zur Loye, H.-C. *Solid State Sci.* **2002**, *4*, 1313. (b) Dong, Y.-B.; Cheng, J.-Y.; Wang, H.-Y.; Huang, R.-Q.; Tang, B.; Smith, M. D.; Huang, R.-Q.; zur Loye, H.-C. *Chem. Mater.* **2003**, *15*, 2593. (c) Dong, Y.-B.; Cheng, J.-Y.; Huang, R.-Q.; Smith, M. D.; zur Loye, H.-C. *Inorg. Chem.* **2003**, *42*, 5699. (d) Dong, Y.-B.; Zhang, Q.; Wang, L.; Ma, J.-P.; Huang, R.-Q.; Shen, D.-Z.; Chen, D.-Z. *Inorg. Chem.* **2005**, *44*, 6591. (e) Dong, Y.-B.; Wang, H.-Y.; Ma, J.-P.; Shen, D.-Z.; Huang, R.-Q. *Inorg. Chem.* **2005**, *44*, 4679. (f) Dong, Y.-B.; Sun, T.; Zhao, X.-X.; Ma, J.-P.; Huang, R.-Q. *Inorg. Chem.* **2006**, *45*, 10613. (g) Dong, Y.-B.; Xu, H.-X.; Ma, J.-P.; Huang, R.-Q. *Inorg. Chem.* **2006**, *45*, 3325. (h) Dong, Y.-B.; Zhang, Q.; Liu, L.-L.; Ma, J.-P.; Tang, B.; Huang, R.-Q. *J. Am. Chem. Soc.* **2007**, *129*, 1514. (i) Dong, Y.-B.; Wang, P.; Ma, J.-P.; Zhao, X.-X.; Tang, B.; Huang, R.-Q. *J. Am. Chem. Soc.* **2007**, *129*, 4872. (j) Wang, P.; Ma, J.-P.; Dong, Y.-B.; Huang, R.-Q. *J. Am. Chem. Soc.* **2007**, *129*, 10620. (k) Hou, G.-G.; Ma, J.-P.; Sun, T.; Dong, Y.-B.; Huang, R.-Q. *Chem.—Eur. J.* **2009**, *15*, 2261. (l) Wang, P.; Ma, J.-P.; Dong, Y.-B. *Chem.—Eur. J.* **2009**, *15*, 10432. (m) Liu, Q.-K.; Ma, J.-P.; Dong, Y.-B. *Chem.—Eur. J.* **2009**, *15*, 10364.

(5) Dong, Y.-B.; Wang, H.-Y.; Ma, J.-P.; Huang, R.-Q. *Cryst. Growth Des.*, **2005**, *5*, 789 and references therein.

Table 1. Crystallographic Data for **L2** and **1**−**3**

compound	**L2**	**1**	**2**	**3**
empirical formula	$C_{12}H_{12}N_6O_3$	$C_{24}H_{30}Cl_3N_{12}O_{21}La$	$C_{24}H_{30}C_{l3}N_{12}O_{21}Pr$	$C_{24}H_{30}C_{l3}N_{12}O_{21}Nd$
fw	288.28	1067.86	1069.86	1073.19
temp (K)	298(2)	298(2)	298(2)	298(2)
cryst syst	monoclinic	orthorhombic	orthorhombic	orthorhombic
space group	*P*2(1)/*c*	*Pccn*	*Pccn*	*Pccn*
a (Å)	14.583(4)	26.835(7)	26.781(3)	26.753(5)
b (Å)	6.4827(17)	6.8826(18)	6.8686(7)	6.8616(11)
c (Å)	13.868(4)	20.754(5)	20.678(2)	20.647(3)
α (deg)	90	90	90	90
β (deg)	107.510(4)	90	90	90
γ (deg)	90	90	90	90
V (Å^3)	1250.2(6)	3833.2(17)	3803.6(7)	3790.1(11)
Z	4	4	4	4
*ρ*calc (g/cm^3)	1.532	1.850	1.868	1.881
F(000)	600	2136	2144	2148
data/restraints/params	2214/0/190	3384/6/286	3363/6/286	3345/6/286
GOF on F^2	1.051	1.098	1.096	1.095
final R indices [$I > 2\sigma(I)$][a]	R1 = 0.0359	0.0433	R1 = 0.0398	R1 = 0.0374
	wR2 = 0.0940	0.1145	wR2 = 0.1168	wR2 = 0.1052

[a] $R1 = \sum||F_o| - |F_c||/\sum|F_o|$. $wR2 = \{\sum[w(F_o^2 - F_c^2)^2]/\sum[w(F_o^2)^2]\}^{1/2}$.

Table 2. Crystallographic Data for **4**−**7**

compound	**4**	**5**	**6**	**7**
empirical formula	$C_{24}H_{30}Cl_3N_{12}O_{21}Sm$	$C_{24}H_{30}C_{l3}N_{12}O_{21}Eu$	$C_{24}H_{30}C_{l3}N_{12}O_{21}Gd$	$C_{24}H_{28}Cl_3N_{12}O_{20}Tb$
fw	1079.30	1080.91	1086.20	1069.85
temp (K)	298(2)	298(2)	298(2)	298(2)
cryst syst	orthorhombic	orthorhombic	orthorhombic	triclinic
space group	*Pccn*	*Pccn*	*Pccn*	$P\bar{1}$
a (Å)	26.743(3)	26.732(3)	26.704(4)	9.2240(16)
b (Å)	6.8506(7)	6.8490(8)	6.8451(9)	11.817(2)
c (Å)	20.586(2)	20.555(2)	20.524(3)	17.362(3)
α (deg)	90	90	90	91.946(2)
β (deg)	90	90	90	94.471(3)
γ (deg)	90	90	90	90.116(3)
V (Å^3)	3771.5(7)	3763.4(8)	3751.7(9)	1885.5(6)
Z	4	4	4	2
*ρ*calc (g/cm^3)	1.901	1.908	1.923	1.884
F(000)	2156	2160	2164	1064
data/restraints/params	3324/0/277	3323/6/286	3321/6/286	6883/12/541
GOF on F^2	1.081	1.078	1.088	1.046
final R indices [$I > 2\sigma(I)$][a]	R1 = 0.0394	R1 = 0.0318	R1 = 0.0337	R1 = 0.0637
	wR2 = 0.0943	wR2 = 0.0842	wR2 = 0.0736	wR2 = 0.1525

[a] $R1 = \sum||F_o| - |F_c||/\sum|F_o|$. $wR2 = \{\sum[w(F_o^2 - F_c^2)^2]/\sum[w(F_o^2)^2]\}^{1/2}$.

1089(vs), 900(s), 808(m), 720(s), 670(s), 626(vs), 567(s), 478(m). Elem anal. (%) calcd for $C_{24}H_{28}Cl_3N_{12}O_{20}Tb$: C 26.94, H 2.64, N 15.71. Found: C 27.01, H 2.69, N 15.62.

Preparation of 8. An aqueous solution (5 mL) of **L2** (13 mg, 0.048 mmol) was gently added to an aqueous solution (5 mL) of $Ho(ClO_4)_3 \cdot 6H_2O$ (26 mg). Upon slow evaporation, colorless block-like crystals (24 mg) were obtained. Yield, 46% (based on **L2**). IR (KBr pellet, cm^{-1}): 3388(s), 1636(s), 1470(s), 1291(m), 1215(s), 1088(vs), 903(s), 812(m), 721(s), 670(s), 627(s), 567(s), 79(w). Elem anal. (%) calcd for $C_{24}H_{28}Cl_3N_{12}O_{20}Ho$: C 26.79, H 2.62, N 15.62. Found: C 26.85, H 2.59, N 15.73.

Preparation of 9. A THF solution (2 mL) of **L2** (13 mg, 0.048 mmol) was gently added to an aqueous solution (2 mL) of $Er(ClO_4)_3 \cdot 6H_2O$ (46 mg). Upon slow evaporation, pink plate-like crystals (23 mg) were obtained. Yield, 45% (based on **L2**). IR (KBr pellet, cm^{-1}): 3395(s), 1636(s), 1521(w), 1470(s), 1408(m), 1359(w), 1291(m), 1215(s), 1088(vs), 901(s), 806(m), 720(s), 669(s), 626(s), 566(s), 482(w). Elem anal. (%) calcd for $C_{24}H_{28}Cl_3N_{12}O_{20}Er$: C 26.74, H 2.62, N 15.59. Found: C 26.67, H 2.74, N 15.44.

Preparation of 10. A MeOH solution (2 mL) of **L2** (26 mg, 0.096 mmol) was gently added to an aqueous solution (2 mL) of $Tm(ClO_4)_3 \cdot 6H_2O$ (90 mg). Upon slow evaporation, colorless block-like crystals (40 mg) were obtained. Yield, 39% (based on **L2**). IR (KBr pellet, cm^{-1}): 3388(s), 1636(s), 1572(w), 1521(w), 1471(s), 1409(w), 1359(w), 1292(m), 1236(s), 1215(s), 1088(vs), 902(s), 807(m), 721(s), 669(s), 626(s), 568(s), 478(m). Elem anal. (%) calcd for $C_{24}H_{28}Cl_3N_{12}O_{20}Tm$: C 26.69, H 2.61, N 15.57. Found: C 26.64, H 2.73, N 15.64.

Preparation of 11. An aqueous solution (5 mL) of **L2** (13 mg, 0.048 mmol) was gently added to an aqueous solution (5 mL) of $Yb(ClO_4)_3 \cdot 6H_2O$ (54 mg). Upon slow evaporation, colorless block-like crystals (21 mg) were obtained. Yield, 40% (based on **L2**). IR (KBr pellet, cm^{-1}): 3390(s), 1635(s), 1521(w), 1471(s), 1291(m), 1215(s), 1090(vs), 904(s), 812(m), 721(m), 670(m), 627(s), 569(s), 479(w). Elem anal. (%) calcd for $C_{24}H_{28}Cl_3N_{12}O_{20}Yb$: C 26.59, H 2.60, N 15.51. Found: C 26.63, H 2.58, N 15.60.

Single-Crystal Structure Determination. Suitable single crystals of **L2** and **1**−**11** were selected and mounted in the air onto thin glass fibers. X-ray intensity data were measured at 293 K on a Bruker SMART APEX CCD-based diffractometer (Mo Kα radiation, $\lambda = 0.71073$ Å). The raw frame data for **L2** and **1**−**11** were integrated into SHELX-format reflection files and corrected for Lorentz and polarization effects using SAINT.[6]

(6) *SAINT*; Bruker Analytical X-ray Systems, Inc.: Madison, WI, 1998.

Table 3. Crystallographic Data for **8-11**

compound	**8**	**9**	**10**	**11**
empirical formula	$C_{24}H_{28}Cl_3N_{12}O_{20}Ho$	$C_{24}H_{28}Cl_3N_{12}O_{20}Er$	$C_{24}H_{28}Cl_3N_{12}O_{20}Tm$	$C_{24}H_{28}Cl_3N_{12}O_{20}Yb$
fw	1075.86	1078.19	1079.86	1083.97
temp (K)	298(2)	298(2)	298(2)	298(2)
cryst syst	triclinic	triclinic	triclinic	triclinic
space group	$P\bar{1}$	$P\bar{1}$	$P\bar{1}$	$P\bar{1}$
a (Å)	9.2387(18)	9.2085(19)	9.2035(13)	9.2282(15)
b (Å)	11.790(2)	11.783(2)	11.7560(16)	11.7514(19)
c (Å)	17.338(3)	17.370(4)	17.331(2)	17.307(3)
α (deg)	92.043(3)	91.881(2)	91.927(2)	91.926(2)
β (deg)	94.711(3)	94.895(3)	94.929(2)	94.975(2)
γ (deg)	90.209(3)	90.418(3)	90.397(2)	90.251(2)
V (Å^3)	1880.8(6)	1876.7(7)	1867.0(4)	1868.7(5)
Z	2	2	2	2
ρcalc (g/cm^3)	1.900	1.908	1.921	1.926
F(000)	1068	1070	1072	1074
data/restraints/params	6863/12/541	6831/0/541	6792/0/442	6807/12/541
GOF on F^2	1.068	1.055	1.046	1.032
final R indices [I > 2σ(I)][a]	R1 = 0.0594	R1 = 0.0564	R1 = 0.0457	R1 = 0.0560
	wR2 = 0.1286	wR2 = 0.1338	wR2 = 0.1096	wR2 = 0.1298

[a] $R1 = \sum||F_o| - |F_c||/\sum|F_o|$. $wR2 = \{\sum[w(F_o^2 - F_c^2)^2]/\sum[w(F_o^2)^2]\}^{1/2}$.

Table 4. Interatomic Distances (Å) for **1**−**6**

1			
La(1)−O(1)	2.471(3)	La(1)−O(5)#2	2.473(3)
La(1)−O(4)	2.596(5)	La(1)−O(2)	2.61(2)
La(1)−O(2)#1	2.605(19)	La(1)−O(3)#1	2.634(4)
2			
Pr(1)−O(2)	2.41(3)	Pr(1)−O(1)	2.437(3)
Pr(1)−O(5)#2	2.439(3)	Pr(1)−O(4)	2.560(5)
Pr(1)−O(3)	2.598(4)		
3			
Nd(1)−O(5)#1	2.423(3)	Nd(1)−O(1)#3	2.427(3)
Nd(1)−O(4)	2.539(5)	Nd(1)−O(2)	2.56(2)
Nd(1)−O(3)	2.579(4)		
4			
Sm(1)−O(1)	2.400(3)	Sm(1)−O(5)#2	2.402(3)
Sm(1)−O(2)	2.483(3)	Sm(1)−O(4)	2.508(5)
Sm(1)−O(3)	2.551(4)		
5			
Eu(1)−O(5)#1	2.390(3)	Eu(1)−O(1)	2.393(3)
Eu(1)−O(4)	2.497(4)	Eu(1)−O(2)	2.51(2)
Eu(1)−O(3)	2.540(3)		
6			
Gd(1)−O(1)	2.383(3)	Gd(1)−O(5)#2	2.385(3)
Gd(1)−O(4)	2.479(4)	Gd(1)−O(2)	2.48(3)
Gd(1)−O(3)#1	2.521(3)		

Table 5. Interatomic Distances (Å) for **7**−**11**

7			
Tb(1)−O(1)#1	2.310(6)	Tb(1)−O(4)	2.313(6)
Tb(1)−O(2)	2.321(7)	Tb(1)−O(3)#2	2.336(6)
Tb(1)−O(6)	2.391(5)	Tb(1)−O(7)	2.400(5)
Tb(1)−O(8)	2.425(5)	Tb(1)−O(5)	2.439(5)
8			
Ho(1)−O(4)	2.283(6)	Ho(1)−O(1)#1	2.291(6)
Ho(1)−O(2)	2.300(6)	Ho(1)−O(3)#2	2.304(6)
Ho(1)−O(6)	2.371(5)	Ho(1)−O(8)	2.389(5)
Ho(1)−O(7)	2.404(5)	Ho(1)−O(5)	2.420(5)
9			
Er(1)−O(4)	2.278(5)	Er(1)−O(1)#1	2.285(6)
Er(1)−O(2)	2.299(6)	Er(1)−O(3)#2	2.302(6)
Er(1)−O(6)	2.363(5)	Er(1)−O(7)	2.377(5)
Er(1)−O(8)	2.395(5)	Er(1)−O(5)	2.405(5)
10			
Tm(1)−O(4)	2.2606	Tm(1)−O(1)#1	2.2725
Tm(1)−O(2)	2.2818	Tm(1)−O(3)#2	2.2846
Tm(1)−O(6)	2.3472	Tm(1)−O(7)	2.3602
Tm(1)−O(8)	2.3679	Tm(1)−O(5)	2.3866
11			
Yb(1)−O(1)#1	2.261(6)	Yb(1)−O(2)	2.267(6)
Yb(1)−O(3)#2	2.282(6)	Yb(1)−O(6)	2.343(5)
Yb(1)−O(8)	2.368(5)	Yb(1)−O(7)	2.375(5)
Yb(1)−O(5)	2.393(5)		

Corrections for incident and diffracted beam absorption effects were applied using SADABS.[6] None of the crystals showed evidence of crystal decay during data collection. All structures were solved by a combination of direct methods and difference Fourier syntheses and refined against F^2 by the full-matrix least-squares technique. Crystal data, data collection parameters, and refinement statistics for **L2** and **1**−**11** are listed in Table 1−3. Relevant interatomic bond distances for **1**−**11** are given in Tables 4 and 5.

Results and Discussion

Ligand. It is demonstrated that the pyridyl-*N*-oxide is a harder donor base than the pyridyl group.[7] As an exobidentate ligand, compared to its pyridyl precursor, **L2** might link to two or more donor centers through the O atom of pyridyl-*N*-oxide owing to the less sterically demanding nature.[8] In addition, **L2** is an oxygen donor ligand, which explains its high affinity to the hard lanthanide cations. As far as we know, some linear and rigid pyridyl-*N*-oxide derivatives, such as 4,4′-bipyridine-*N*,

(7) (a) Hill, R. J.; Long, D.-L.; Champness, N. R.; Hubberstey, P.; Schröder, M. *Acc. Chem. Res.* **2005**, *38*, 337. (b) Loeb, S. J. *Chem. Commun.* **2005**, 1511. (c) Hoffart, D. J.; Loeb, S. J. *Angew. Chem., Int. Ed.* **2005**, *117*, 901. (d) Dalgarno, S. J.; Hardie, M. J.; Atwood, J. L.; Warrenc, J. E.; Raston, C. L. *New J . Chem.* **2005**, *29*, 649.

(8) (a) Mantero, D. G.; Neels, A.; Helen, S.-E. *Inorg. Chem.* **2006**, *45*, 3287. (b) Zhang, L.-P.; Lu, W.-J.; Mak, T. C. W. *Chem. Commun.* **2003**, 2830. (c) Mantero, D. G.; Neels, A.; Stoeckli-Evans, H. *Inorg. Chem.* **2006**, *45*, 3287.

Scheme 1. Synthesis of Symmetric and Asymmetric Oxadiazole-Bridged *N*,*N*′-Dioxide Ligands **L2** and **L3**

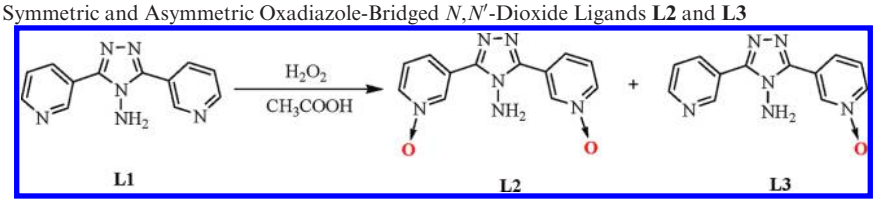

N′-dioxide, pyrazine-*N*,*N*′-dioxide, 1,2-bis(pyridin-4-yl)-ethane-*N*,*N*′-dioxide, and *trans*-1,2-bis(pyridin-4-yl)ethene-*N*,*N*′-dioxide, have been employed as organic building blocks in self-assembly reactions with various metal centers.[7,8]

L2 was expediently synthesized by the oxidation of L1 with H_2O_2 in the presence of CH_3COOH in a moderate yield. In addition, an asymmetric oxidation product of **L3** was also isolated from the reaction as a byproduct (Scheme 1). **L3** with different terminal coordination functional groups might be an ideal candidate to synthesize heterometallic complexes. **L2** and **L3** are soluble in common polar organic solvents such as CH_2Cl_2, $CHCl_3$, MeOH, EtOH, and H_2O, which facilitates the reactions between them with metal ions in solutions. Besides ^1H NMR, IR, and elemental analyses, the structure of **L2** was further confirmed by X-ray single crystal diffraction in the solid state. As shown in Figure 1, the backbone of **L2** is bent, which is similar to that of **L1**. It is noteworthy that two pyridyl-*N*-oxide moieties attached to the central triazole via an exotriazole C−C single bond at the 2,5-positions to create the bent spacer, in which two pyridyl-*N*-oxide moieties can rotate freely around the single C−C bond, which results in the flexibility of **L2**. Scheme 2 presents three possible typical conformations of **L2**. In the solid state, **L2** adopts conformation III, in which the two terminal pyridyl-*N*-oxide groups are transoid. The separation between two terminal O atoms is ca. 11 Å, which is ca. 2 Å longer than that of **L1**.[5]

Ln(III)-Based Coordination Polymers. Synthesis. All the Ln(III)−**L2** polymers were synthesized by the combination of **L2** with an excess of $Ln(ClO_4)_3 \cdot 6(H_2O)$ in water at room temperature. It is worthwhile to point out that, in these specific reactions, the products do not depend on the metal-to-ligand ratio. However, increasing the metal-to-ligand ratio resulted in somewhat higher yield and higher crystal quality. The crystals suitable for X-ray single crystal analysis were grown by slow evaporation from aqueous solution. Interestingly, under the same experimental conditions, the combination of $Ln(ClO_4)_3 \cdot 6(H_2O)$ with **L2**, however, generated two series of Ln(III)−**L2** polymers with distinctly different structural features, which is certainly caused by the different conformation adopted by **L2** in the solid state. As shown in Scheme 3, **L2** adopts conformation II in **1**−**6** and conformation I in **7**−**11**. Although we distance ourselves from any type of explanation and say forthright that we do not know the function of the f-block metal perchlorate salts in the formation of **1**−**6** and **7**−**11**, nevertheless, it appears the sizes of the f-block metal ions used in this synthesis are critical in influencing the product structure.[9]

(9) (a) Parker, D.; Puschmann, H.; Batsanov, A. S.; Senanayake, K. *Inorg. Chem.* **2003**, *42*, 8646. (b) Li, X.; Liu, W.; Guo, Z.; Tan, M. *Inorg. Chem.* **2003**, *42*, 8735.

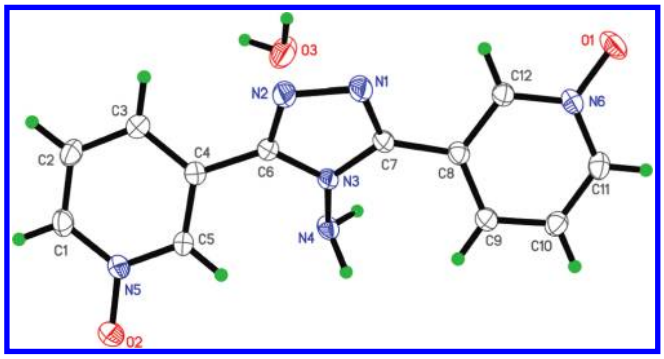

Figure 1. The ORTEP figure of **L2** (displacement ellipsoids drawn at 30% probability level).

Structural Analysis. Compounds 1−**6.** The X-ray crystal structure analysis revealed that **1**−**6** are isostructural. They crystallize in the orthorhombic space group *Pccn*. Therefore, only the structure of **4** is described in detail herein. As shown in Figure 2, each Sm1 node adopts a distorted single-capped square antiprism coordination sphere.[8c] The square antiprism is defined by eight carboxylic oxygen donors with Sm−O distances ranging from 2.400(3) to 2.508(5) Å, which are comparable to those reported for other nine-coordinated Sm−oxygen complexes.[10] The apical coordination water molecule is in a sterically demanding position, which leads to a relative lengthening of the Ln−OH_2 bond at 2.551(4) Å.[11a] It is noteworthy that the Sm(III) ion and one perchlorate (Cl(2)) are located on a crystallographic 2-fold axis, and the other (Cl(1)) is at a general position.

In **4**, **L2** acts as a bidentate ligand to bind Sm(III) cations into a noninterpenetrating two-dimensional network, in which ligand **L2** adopts the conformation II. The separation between two terminal O atoms is ca. 11 Å, which is comparable to that of conformation III. Each ligand bonds to two Sm(III) cations via the two terminal oxygen atoms, while in turn each Sm(III) cation coordinates to four ligands. The ligands bridge to create one-dimensional chains of cations connected by terminal *N*-oxide moieties. These one-dimensional chains are double-stranded and extend along the crystallographic *b* axis and further cross-link through the Sm(III) nodes into a two-dimensional net (Figure 3). A side view of the two-dimensional net is "double-edged" due to the involved helical chains. As shown in Figure 3, the double-stranded chains are not one-handed, in which *P* and *M* helices are held together by interchain hydrogen bonds to create the tube with an ellipse-like channel with a diameter of ca. 10 Å. The

(10) Hoffart, D. J.; Loeb, S. J. *Angew. Chem., Int. Ed.* **2005**, *44*, 901.
(11) (a) Muniappan, S.; Lipstman, S.; George, S.; Goldberg, I. *Inorg. Chem.* **2007**, *46*, 5544. (b) Wang, J.; Wang, R.; Yang, J.; Zheng, Z.; Carducci, M. D.; Cayou, T.; Peyghambarian, N.; Jabbour, G. E. *J. Am. Chem. Soc.* **2001**, *123*, 6179.

Scheme 2. Three Typical Possible Conformations of **L2**

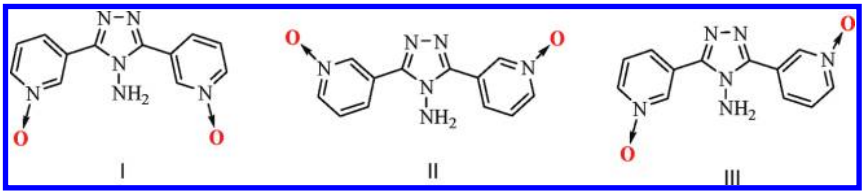

Scheme 3. Synthesis of Ln(III)-Based Coordination Polymers **1**−**6** and **7-11** Based on **L2**

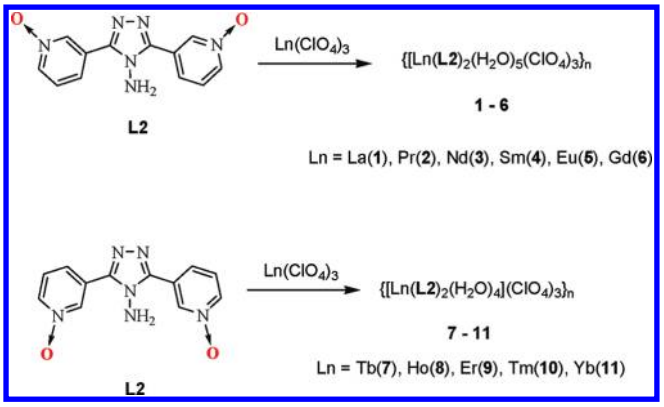

hydrogen bonding system consists of two adjacent water molecules on two Sm(1) atoms from the *P* and *M* helices. As shown in Figure 4, the O(2)···H(2B) and O(2)···O(2) distances are 1.886(7) and 2.815(7) Å, respectively. The corresponding O(2)···H(2B)−O(2) angle is 172.5(3)°. The helical pitch, given by the distance between equivalent atoms results from one complete rotation of the 2-fold screw axis, is ca. 13.7 Å. The first kind of ClO_4^- anions are encapsulated inside and hydrogen-bonded to the coordinated water molecules on the adjacent Sm(1) centers (Figure 4).

The second kind of ClO_4^- anion is located between the layers. The two-dimensional nets of **4** have close neighboring nets resulting from internet hydrogen-bonding interactions via a ClO_4^- bridge. The hydrogen-bonding system consists of a ClO_4^- anion, a $-NH_2$ group on the ligand, and a H_2O molecule on the Sm1 atom. As shown in Figure 5, the O(6)···H(5) and O(7)···H(3B) distances are 2.506 (7) and 1.971(6) Å, respectively. The O(6)···N(5) and O(3)···O(7) distances are 3.270(8) and 2.803(6) Å, respectively. The O(6)···H(5)−N(5) and O(7)···H(3B)−O(3B) angles are 144.7(3) and 167.4(6)°, respectively. These internet hydrogen-bonding interactions give rise to a three-dimensional arrangement (Figure 5).

For **1**−**6**, the ligand donor to Ln(III) bond lengths simply reflects the ionic radius variation. The Ln−$O_{N\text{-oxide}}$ bond lengths decrease regularly by 0.086 Å from La(III) to Gd(III). The cell volume from **1** to **6**, as shown in Table 1, also faithfully follows the same trend and decreases by 81.5 $Å^3$.

Compounds 7−**11.** Compounds **7**−**11** are isostructural, and they all crystallize in the triclinic space group $P\bar{1}$. Therefore, only the structure of **7** is described in detail herein. X-ray single crystal structural analysis revealed that there is only one crystallographic Tb(III) center in **7**. It coordinates to four pyridyl-*N*-oxides of bridging **L2** and to four water molecules (Figure 6). The coordination geometry around the Tb1 center is an irregular eight-coordination sphere. The Tb−O (*N*-oxide) bond distances range from 2.310(6) to 2.336(6) Å, and that of the Tb−O (aqua) bond is from 2.391(5) to 2.439(5) Å, all of which are within the range of those reported for other eight-coordinate Tb(III) complexes with oxygen donors.[11b]

Notably, differently than in compounds **1**−**6**, **L2** adopts conformation I in **7**−**11**. The separation between two terminal O atoms is ca. 9.3 Å, which is shorter than those of conformations II and III. In addition, **L2** is not planar but twisted, and the dihedral angle between the two terminal pyridyl rings is 47.1(6)°. As shown in Figure 7, the twisted **L2** adopts a *cis* conformation to link the Tb(III) ions to form a double helix along the crystallographic *b* axis, in which two helical strands are of the same chirality (Figure 7a). The chiral double-stranded helix is hydrogen bonded to its neighbors, which adopt the different chirality. The two triazole nitrogen atoms act as the hydrogen bond acceptors, forming two N···H−O (O(8)−H(8B)···N(10) and O(7)−H(7B)···N(9)) hydrogen bonds between two coordination water molecules on the Tb(III) atom of its neighbor chains to create a two-dimensional hydrogen-bonded net extended in the crystallographic *bc* plane. The N(9)···H and N(10)···H distances are 1.87(5) and 2.02(5) Å. The N(9)···O(7) and N(10)···O(8) contacts are 2.714(9) and 2.833(9) Å, and the corresponding O(7)−H(7B)···N(9) and O(8)−H(8B)···N(10) angles are 171.1(4) and 160.4(5)°, respectively. The alternative arrangement of *P* and *M* double-stranded chains leads to an achiral compound. The uncoordinated ClO_4^- counterions are located between these layers and further are hydrogen bonded to the layers through O(7)−H(7A)···O(12) (H···O(12) = 2.35(5) Å, O(7)···O(12) = 3.06(2) Å, and ∠O(7)−H(7A)···O(12) = 141.6(6)°) and O(5)−H(5B)···O(9) (H···O = 2.21(5) Å, O(5)···O(9) = 2.973(14) Å, and ∠O(5)−H(5B)···O(9) = 149.5(6)°) bonds to generate a three-dimensional network (Figure 8).

Similarly to **1**−**6**, the same structural variation is observed for **7**−**11** due to the lanthanide contraction. The Ln−$O_{N\text{-oxide}}$ is reduced regularly from 2.291(6) to 2.261(6) Å, and the corresponding cell volume decreases from 1885.5(6) to 1868.7(5) $Å^3$. In addition, the structural difference between **1**−**6** and **7**−**11** clearly results from the lanthanide contraction. The La(III), Pr(III), Nd(III), Sm(III), Eu(III), and Gd(III) cations with larger ionic radii adopt a nine-coordinate $\{LnO_9\}$ sphere, whereas the Tb(III), Ho(III), Er(III), Tm(III), and Yb(III) cations with smaller ionic radii lie in a $\{LnO_8\}$ coordination environment clearly due to the steric demand.[9b]

Luminescent Properties. The lanthanide complexes with distinct luminescent properties are currently of interest for use in applications involving the fabrication

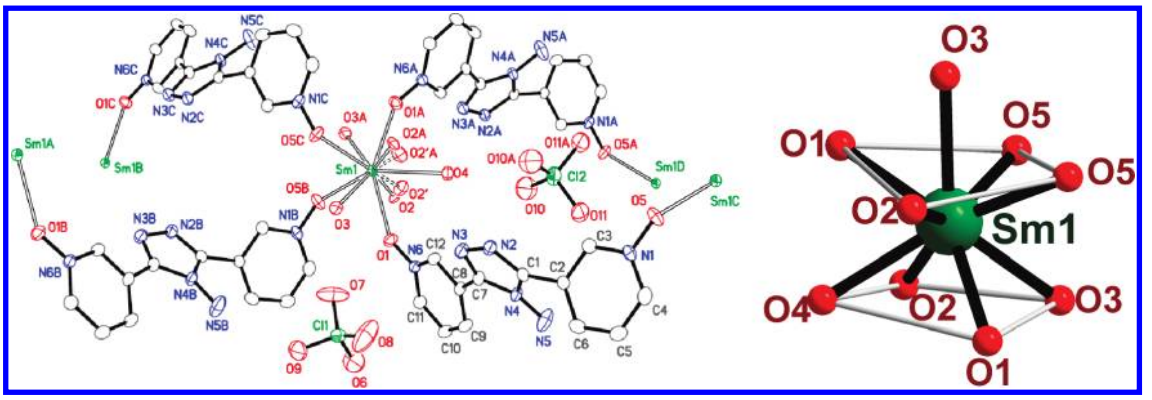

Figure 2. The ORTEP figure of compound **4** (left) and its distorted monocapped square-antiprismatic coordination sphere (right).

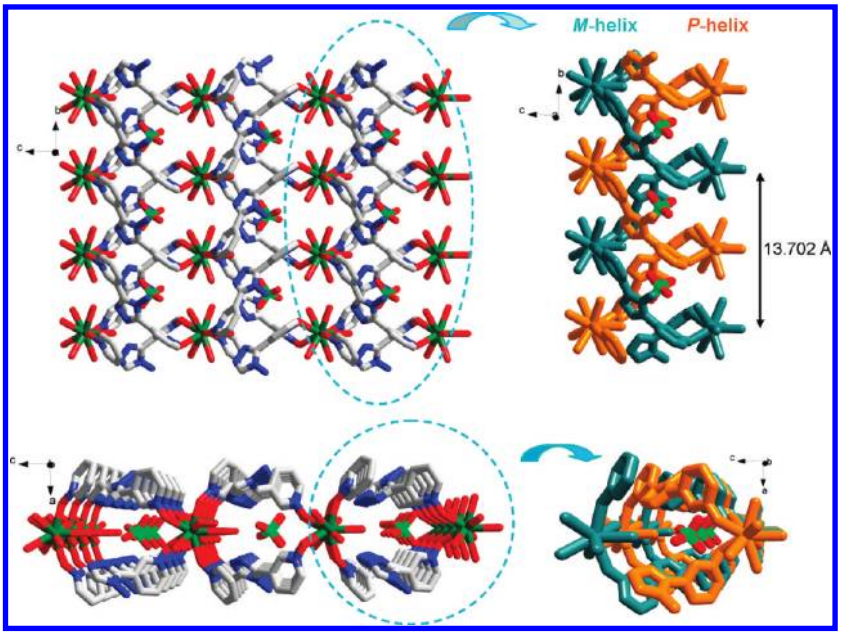

Figure 3. Top (up) and side (bottom) views of the two-dimensional Sm(III) net consisting of *P* and *M* helices in **4**.

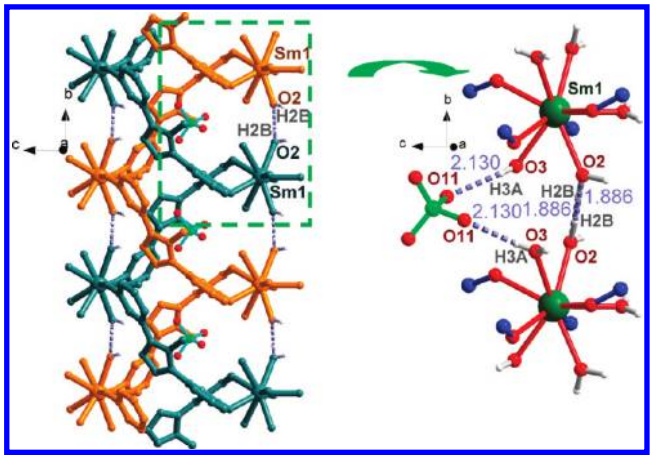

Figure 4. *P* and *M* helices hydrogen-bonded together in **4** to generate channels which contain ClO_4^- anions.

of novel materials.[12] As attractive NIR and visible-light emitting luminescent centers, Nd(III),[13] Eu(III),[14] and Tb(III)[14] complexes were chosen to investigate the luminescence in the solid state. For **3**, two sharp emission peaks were observed in the NIR range upon excitation at 800 nm. As shown in Figure 9, the emission bands observed at 1057 (prominent line) and 1336 nm are attributed to the $^4F_{3/2} \rightarrow {}^4I_{11/2}$ and $^4F_{3/2} \rightarrow {}^4I_{13/2}$ transitions of Nd(III), respectively. For **5**, the emission bands arise from the $^5D_0 \rightarrow {}^7F_J$ (J = 1, 2, 3, 4) transitions of Eu(III). The corresponding emission bands are 591, 612, 649, and 695 nm, respectively, upon excitation at 395 nm. Among these transitions, $^5D_0 \rightarrow {}^7F_2$ is the strongest. For **7**, upon excitation at 302 nm, four lines of Tb(III) emission can be detected in the visible spectrum, corresponding

(12) (a) Petoud, S.; Muller, G.; Moore, E. G.; Xu, J.; Sokolnicki, J.; Riehl, J. P.; Le, U. N.; Cohen, S. M.; Raymond, K. N. *J. Am. Chem. Soc.* **2007**, *129*, 77. (b) Seitz, M.; Moore, E. G.; Ingram, A. J.; Muller, G.; Raymond, K. N. *J. Am. Chem. Soc.* **2007**, *129*, 15468. (c) Yang, X.; Jones, R. A. *J. Am. Chem. Soc.* **2005**, *127*, 7686. (d) Chatterton, N.; Bretonnière, Y.; Pécaut, J.; Mazzanti, M. *Angew. Chem., Int. Ed.* **2005**, *44*, 7595. (e) Bekiari, V.; Pistolis, G.; Lianos, P. *Chem. Mater.* **1999**, *11*, 3189. (f) Tremblay, M. S.; Halim, M.; Sames, D. *J. Am. Chem. Soc.* **2007**, *129*, 7570.

(13) (a) Halim, M.; Tremblay, A. S.; Jockusch, S.; Turro, N. J.; Sames, D. *J. Am. Chem. Soc.* **2007**, *129*, 7704. (b) Zhang, J.; Badger, P. D.; Geib, S. J.; Petoud, S. *Angew. Chem., Int. Ed.* **2005**, *44*, 2508.

(14) Johansson, M. K.; Cook, R. M.; Xu, J.; Raymond, K. N. *J. Am. Chem. Soc.* **2004**, *126*, 16451.

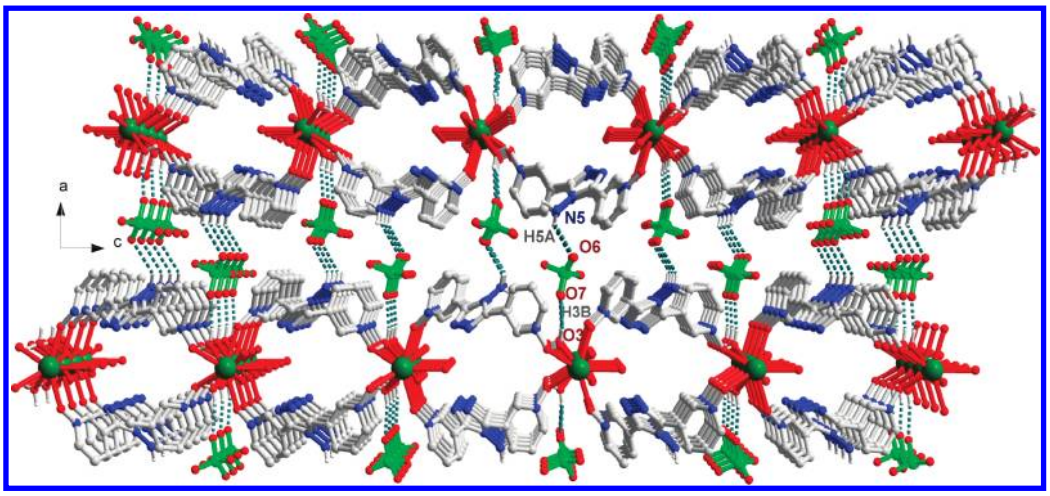

Figure 5. Three-dimensional H-bonded network of **4** in the solid state. The first type of ClO_4^- anion in the channels is omitted for clarity.

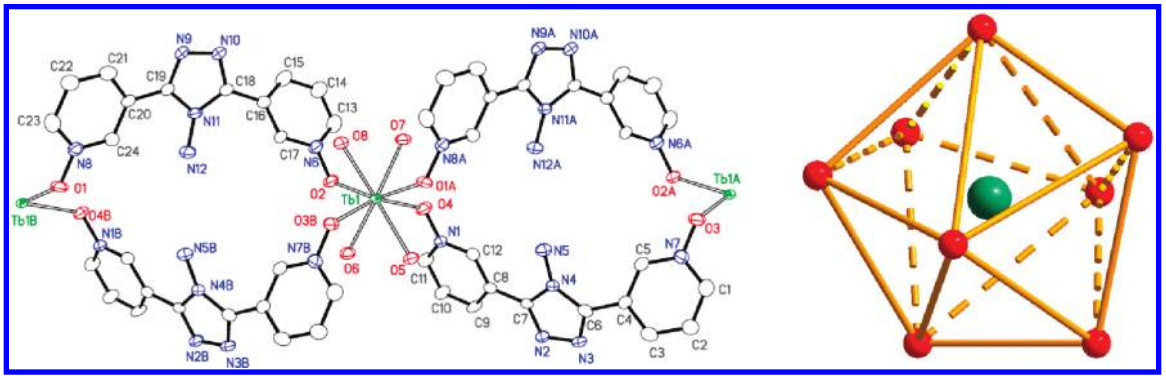

Figure 6. The ORTEP figure of **7** (left) and its irregular eight-coordination sphere (right).

to transitions from the $^5D_4$ state: $^5D_4 \rightarrow {}^7F_6$ (487 nm), $^5D_4 \rightarrow {}^7F_5$ (543 nm), $^5D_4 \rightarrow {}^7F_4$ (585 nm), and $^5D_4 \rightarrow {}^7F_3$ (619 nm). The most prominent line was observed at 543 nm.

As shown in the Structural Analysis section, all of the Ln(III) complexes herein contain coordinated water molecules. It is well-known that the O−H oscillators on these water molecules are effective quenchers for the f−f luminescence.[15] In previous studies, chemists tried to reduce the O−H variation by changing O−H to O−D or O−F or removing the water molecules from the compound to enhance the luminescent intensity of the Ln(III) species containing coordinated water molecules.[15] It is noteworthy to point out that the coordination water molecules on Ln(III) in **1**−**11** are hydrogen-bonded to the hydrogen binding acceptors around them, including ClO_4^-, the triazole ring, and coordination water molecules on adjacent Ln(III) centers (Figure 10); thus, the vibronic deactivation resulting from the O−H oscillators on the coordinated water molecules is efficiently avoided, consequentially leading to the strong luminescence in the solid state.[16]

Recently, our research group has provided a series of lanthanide-based discrete and polymeric host−guest systems $[Ln(H_2O)_8]^{3+} \subset Ln^{III}{}_2L_4$ assembled from lanthanide cations and a bent 1,2,4-triazole-bridged organic ligand.[4i,j,l] The luminescent colors within the UV−vis and UV−vis/NIR regions of these supramolecular host−guest systems can therefore be tuned by controlling the types of the encapsulated guest species via reversible solid-state f−f lanthanide cation exchange. In addition, the luminescent intensity can also be tuned on the basis of the solid-state f−d transition metal exchange.[4l] As mentioned above, the counterion ClO_4^- anions in compounds **3**, **5**, and **7** serve as important hydrogen bond acceptors to fix the O−H oscillators on the coordination water molecules, which play a key role in ensuring the luminescent intensity. We wonder if the luminescent intensity could be tuned by controlling the involved counterions, that is, replacing the strong hydrogen bond acceptor of ClO_4^- with another weak hydrogen bond acceptor such as halogen anions to release the O−H oscillators. With this in mind, the solid-state anion exchange was performed on compound **7** with weak hydrogen bond acceptor I^-. As expected, when the crystals of **7** were treated by an excess of NaI in an EtOH medium at room temperature, the luminescent intensity of Tb(III) gradually decreased as time progressed. As shown in Figure 11, the Tb(III)-centered luminescent intensity was depressed after 4 h. Thus, the strong luminescence originating from **7** could be effectively quenched via this anion-driven approach. After 8 h, the solid-state emission spectra of the resulting crystalline solids did not appear to change with time, indicating that the guest exchange reaction of ClO_4^- by I^- is

(15) (a) Kłonkowski, A. M.; Lis, S.; Pietraszkiewicz, M.; Hnatejko, Z.; Czarnobaj, K.; Elbanowski, M. *Chem. Mater.* **2003**, *15*, 656. (b) Wong, K.-L.; Law, G.-L.; Yang, Y.-Y.; Wong, W.-T. *Adv. Mater.* **2006**, *18*, 1051.

(16) Jiang, Y.-Y.; Ren, S.-K.; Ma, J.-P.; Liu, Q.-K.; Dong, Y.-B. *Chem.—Eur. J.* **2009**, *15*, 10742.

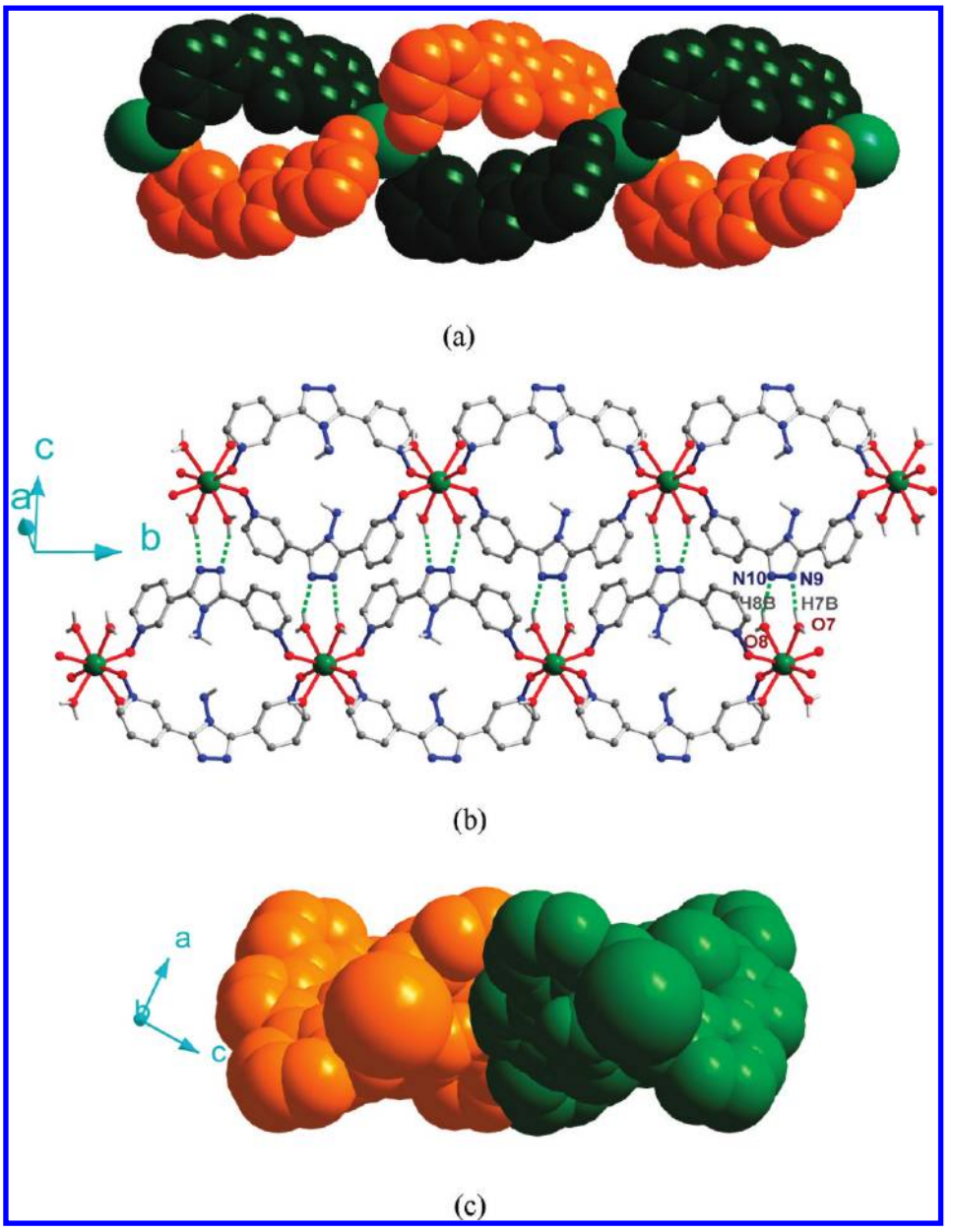

Figure 7. Structural description of **7**. (a) Double-stranded helical chain with only one-handedness. (b) Interchain hydrogen bonding systems. (c) Top view of two adjacent double-stranded chains with different handedness.

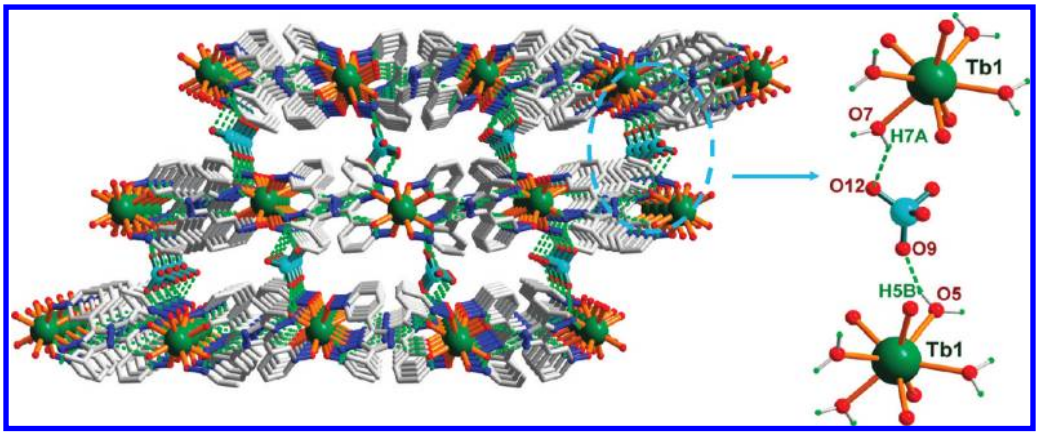

Figure 8. Three-dimensional hydrogen-bonded network linked by the $Tb(H_2O)\cdots ClO_4^-\cdots Tb(H_2O)$ linkage in **7**.

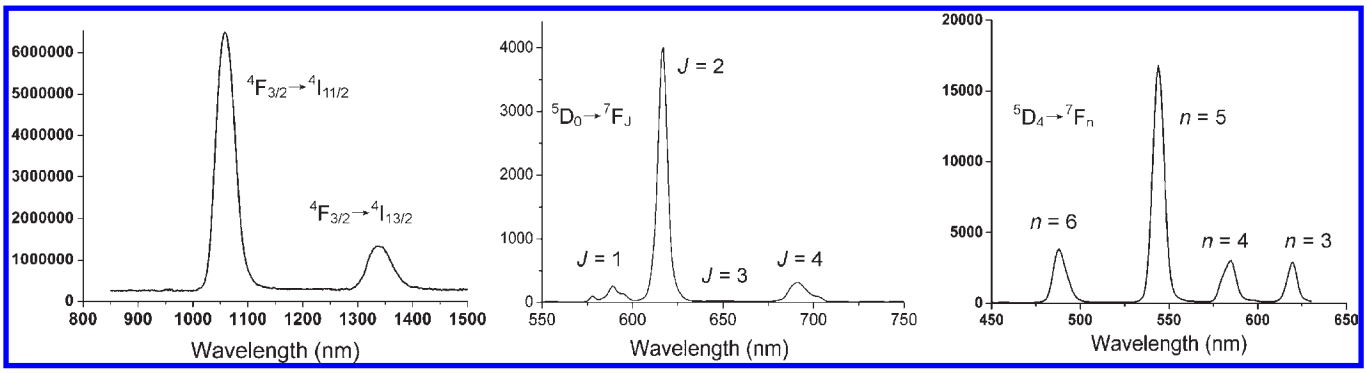

Figure 9. The solid state emission spectra of **3** (left), **5** (middle), and **7** (right).

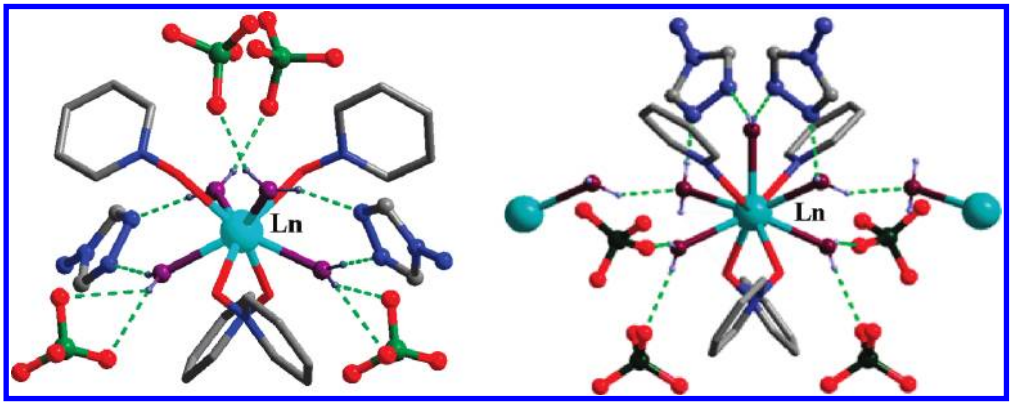

Figure 10. The hydrogen bonding systems around the coordination water molecules in **1**−**6** (left) and **7**−**11** (right).

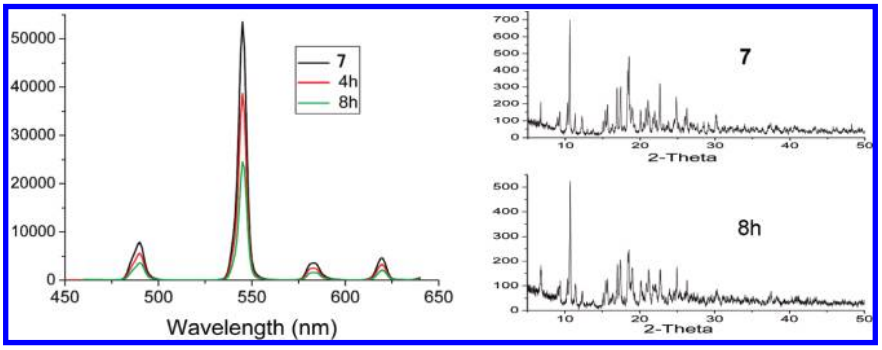

Figure 11. Left: The solid-state emission spectra of compound **7** (λ_{ex} = 302 nm, black line) and the solid-state emission spectra (λ_{ex} = 302 nm) of **7** stirred in an EtOH solution of NaI (excess) for 4 and 8 h (red and green lines, respectively). Right: The X-ray powder diffraction patterns corresponding to **7**, which was stirred in an EtOH solution of NaI (excess) for 8 h, respectively.

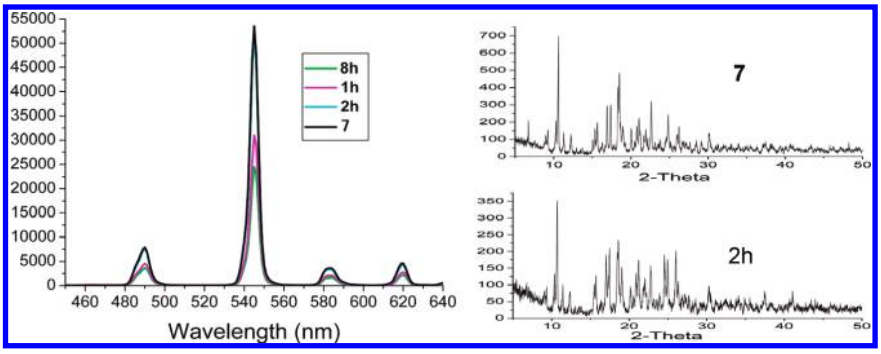

Figure 12. Left: The solid-state emission spectra of compound **7** (λ_{ex} = 302 nm, black line), the solid-state emission spectra (λ_{ex} = 302 nm, green line) of the sample, which was **7** stirred in an EtOH solution of NaI (excess) for 8 h, and the solid-state emission spectra (λ_{ex} = 302 nm) of the sample (represented by green line) stirred in $NaClO_4$ (excess) for 1 and 2 h (purple and cyan lines, respectively). The cyan line is largely overlapped by the black line. Right: The X-ray powder diffraction patterns corresponding to **7**. The sample (represented by green line) was stirred in an EtOH solution of $NaClO_4$ (excess) for 2 h.

basically in equilibrium. The XRPD monitoring demonstrates that the structure of **7** is maintained during the course of the anion-exchange reaction (Figure 11). Interestingly, upon addition of ClO_4^-, the luminescent intensity of **7** was recovered back to its original state only after 2 h (Figure 12), reflecting that the displacement rate of I^- by ClO_4^- is much faster than that of ClO_4^- by I^-. Hence, the porous network shows interesting reversibility for anion inclusion. It is reasonable to suggest that this emission intensity can be reduced upon replacement of the strong hydrogen bond acceptor of ClO_4^- by the weak hydrogen bond acceptor of I^-, which releases the fixed O−H oscillators and partially recovers their vibration. So the luminescent intensity of the lanthanide-centered emitters herein can be tuned by controlling the involved anions, which could serve as a significant complement to the growing field of guest-driven luminescence.[4i,j,l,16]

Conclusions

In conclusion, a new bent 1,2,4-triazole-bridged *N*,*N*′-dioxide, **L2**, was designed and synthesized by the oxidation of 3,5-bis(3-pyridyl)-4-amino-1,2,4-triazole with H_2O_2 in the presence of HOAc at ambient temperature. Eleven Ln(III)-based coordination polymers have been successfully prepared by the solution reactions of **L2** with various Ln(III)−perchlorates. The structures of these new Ln(III) polymers clearly reflect the effect of the lanthanide contraction. For the compounds **1**−**6**, the Ln(III) atoms adopt a nine-coordinate $\{LnO_9\}$ sphere because of their larger ionic radii, whereas the Ln(III) centers in compounds **7**−**11** with smaller ionic radii lie in a $\{LnO_8\}$ coordination environment. In addition, all the coordination water molecules in the reported complexes are firmly fixed by the strong hydrogen bonding interactions. Thus, the vibration moment of the O−H oscillator, being an efficient quencher for the f−f luminescence, is effectively reduced. Consequently, compound **3** presents a strong emission in the NIR region, whereas **5** and **7** exhibit strong red and green emissions within the UV−vis region, respectively. More importantly, the emission intensity, for example **7**, can be reversibly tuned by controlling the type of involved counterion. Such reversible solid-state anion exchange might provide an alternative approach to tuning the luminescence and, furthermore, some applications in sensors and switches.

Acknowledgment. This work was supported by the National Natural Science Foundation of China (Grant No. 20871076), Shangdong Natural Science Foundation (Grant No. JQ200803), and Ph.D. Programs Foundation of Ministry of Education of China (Grant No. 200804450001).

Supporting Information Available: Crystallographic data are available as a CIF file. This material is available free of charge via the Internet at http://pubs.acs.org.